CrossMark

ORIGINAL PAPER

Effects of various combinations of boundary layer schemes and microphysics schemes on the track forecasts of tropical cyclones over the South China Sea

Shumin Chen[1] · Yu-Kun Qian[1] · Shiqiu Peng[1]

Abstract This study investigates the effects of various combinations of the planetary boundary layer (PBL) schemes and the microphysics schemes on the numerical forecasting of tropical cyclones (TCs). Using different combinations of three PBL schemes (YSU, MYJ and MYNN2) and four microphysics schemes (Ferrier, Goddard, WSM6 and Lin), a number of experiments are carried out for five landed TCs in the South China Sea during 2012. Results show that the combination of the YSU and Ferrier schemes performs the best for the TC track forecasting, although it does not perform the best for the forecast of precipitation. Further analysis reveals that the best performance of the track forecast by the combination of the YSU and Ferrier schemes mainly attributes to a more accurate steering flow as well as TC wind structure produced by this combination. These results provide a valuable reference to the operational numerical forecasting of TC tracks in the future.

1 Introduction

Tropical cyclones (TCs) are one of the most destructing natural hazards (Emanuel 2005; Peng et al. 2014) and pose great scientific challenges to meteorologists. The planetary boundary layer (PBL) scheme and the microphysics scheme have been shown critical to the numerical forecasting of TCs, because the boundary layer processes regulate the sources of heat and moisture, and sink of momentum in TCs (Kepert 2012), while the cloud


✉ Shiqiu Peng
speng@scsio.ac.cn

[1] State Key Laboratory of Tropical Oceanography, South China Sea Institute of Oceanology, Chinese Academy of Sciences, 164 West Xingang Road, LTO/SCSIO, Guangzhou 510301, China

dynamical properties such as vertical velocity and cloud top height are determined by the microphysics scheme in numerical models (Khain and Lynn 2011).

Many studies focus on the effects of single PBL scheme (e.g., Rao and Prasad 2007; Kanada et al. 2012; Kepert 2012) or single microphysics scheme (e.g., Wang 2002, Khain and Lynn 2011; Pattanayak et al. 2012). However, effects by various combinations of PBL and microphysics schemes have only received limited attentions. Indeed, interactions between the PBL and the microphysical processes cannot be overlooked. On one hand, the condensation processes in PBL have interactions with the microphysics in clouds (Nakanishi 2000, 2001; Nakanishi and Niino 2004, 2006). On the other hand, the downward short-wave and long-wave radiations to PBL are governed by the cloud effects in microphysics schemes. Hence, various combinations of PBL and microphysics schemes may have different influences on TC simulations and forecasts. Study from Zhou et al. (2013) shows that the combination of YSU scheme (the Yonsei University PBL scheme, Hong et al. 2006) and Ferrier scheme (the Eta Grid-scale Cloud and Precipitation scheme, Ferrier et al. 2002) is the best choice for the track simulation of super Typhoon Megi (201013). However, this study may be case-dependent because only one TC was analyzed. In the present study, an ensemble of forecasting experiments using different combinations of PBL and microphysics schemes are carried out for five TCs in the South China Sea (SCS), one of the major active regions of TCs (Chen et al. 2014), to figure out the effects by various combinations of PBL and microphysics schemes on the track forecasts.

The present study is organized as follows. Sections 2 and 3 present the forecasting experiments with different combinations of physical schemes and analysis results, repectively. Conclusions and discussions are given in the final section.
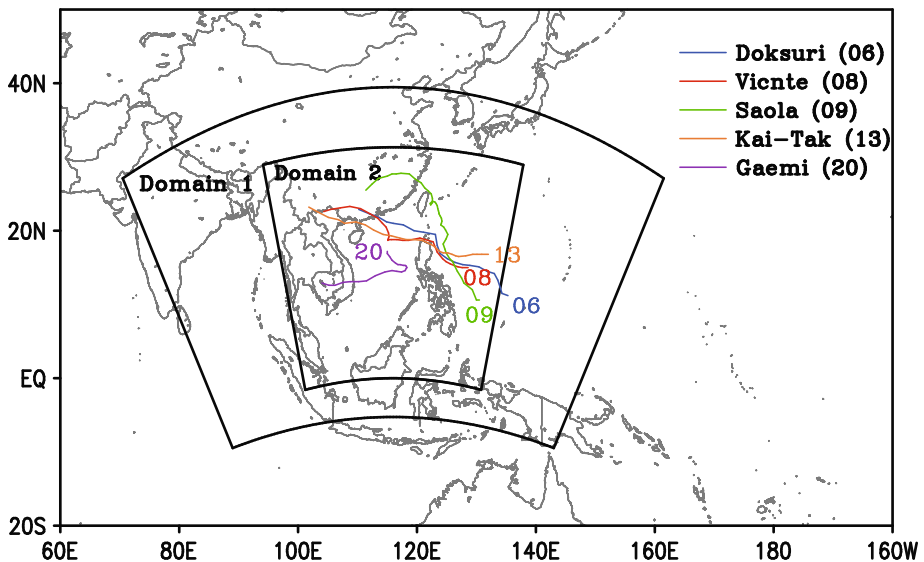
Fig. 1 Model domains of WRF and the JTWC best tracks of the five selected TCs in 2012

2 The forecasting experiments

The experiments carried out in this study are based on the Weather Research and Forecasts (WRF) model (Skamarock et al. 2008), developed by the National Center for Atmospheric Research (NCAR) and the National Centers for Environmental Prediction (NCEP) in the USA. It is a next-generation meso-scale model for advancing the understanding and prediction of meso-scale weather and accelerating the transfer of research advances into operations. A dynamical downscaling technique is employed to obtain higher-resolution output with small- and meso-scale features from the lower-resolution output of a global atmospheric model. To realize this, a two-domain-one-way-nested configuration is designed, as shown in Fig. 1. The outer domain for the atmospheric model covers the Western North Pacific (WNP), the entire SCS, and the eastern Indian Ocean, with a horizontal grid resolution of 72 km. The inner domain covers the entire SCS and southern China, with a horizontal grid resolution of 24 km. Both domains have 27 layers in the vertical. The output from the Global Forecast System (GFS) maintained by NCEP with horizontal grid resolution of 1° × 1° is used to provide initial conditions and lateral boundary conditions for the outer domain. The Kain-Fritsch cumulus scheme (Kain and Fritsch 1990, 1993), Dudhia shortwave (Dudhia 1989) and RRTM longwave (Mlawer et al. 1997) radiation scheme are chosen for both domains.

An ensemble of experiments using different combinations of three PBL schemes and four microphysics schemes are carried out. The three PBL schemes are the YSU scheme, the MYJ scheme (the Mellor-Yamada-Janjić PBL scheme, Janjić 1994) and the MYNN2 scheme (the Level 2.5 Mellow-Yamada Nakanishi Niino PBL scheme, Nakanishi and Niino 2006), while the four microphysics schemes are the Ferrier scheme, the Goddard scheme (the Goddard Cumulus Ensemble Model scheme, Tao et al. 1989), the WSM6 scheme (the WRF Single-Moment 6-class scheme, Hong and Lim 2006) and the Lin scheme (the Purdue Lin scheme, Lin et al. 1983), respectively. In order to reduce case dependence, five TCs that entered the inner domain of the model during 2012 are selected. In the WRF model, the surface environments are similar over the sea and varied over the continent, hence the effects by the PBL schemes are more significant near or on the continent. Thus, in order to enlarge the effects of the PBL schemes, the selected TCs should have made landfall. The TCs chosen for this analysis are Doksuri (201206), Vicnte (201208), Saola (201209), Kai-Tak (201213) and Gaemi (201220), respectively. Their observed tracks produced by Joint Typhoon Warning Center (JTWC, http://www.usno.navy.mil/JTWC/) are also shown in Fig. 1. The forecasting experiments are initialized at 72, 48 and 24 h before the landing of each TC. There are totally eighteen initialization times, six for Typhoon Kai-Tak, which landed for two times, and three for every other TCs.

3 Results from the experiments

3.1 The tracks

Based on the observed tracks produced by JTWC, the track position error (TPE) for 24-, 48- and 72-h forecasts by each combination of PBL and microphysics schemes is calculated using the following formula (Neumann and Pelissier 1981; Powell and Aberson 2001):

$$\text{TPE} = 111.11 \frac{180}{\pi} \cos^{-1}[\sin \varphi_O \sin \varphi_S + \cos \varphi_O \cos \varphi_S \cos(\lambda_O - \lambda_S)], \qquad (1)$$

where λ_O and φ_O are the longitude and latitude of the observed storm center, and λ_S and φ_S are those of the storm center forecasted by each combination. Further, in order to make a relative comparison between different combinations of physics schemes, the relative error (R_i) of each TC track predicted by each combination is calculated using the following formula:

$$R_i = \frac{\text{TPE}_i}{\overline{\text{TPE}}} \qquad (i = 1\ldots,N), \qquad (2)$$

where $\overline{\text{TPE}} = \frac{1}{N}\sum_{i=1}^{N} \text{TPE}_i$ and N denotes the number of combinations.

The mean TPEs and the relative error of various combinations, which is averaged over the ensemble forecasts for five selected TCs, are listed in Table 1. The combination of YSU and Ferrier schemes gets the smallest TPE and relative error for 24- and 72-h forecasts, while it ties the combination of MYNN2 and Lin schemes for the best in 48-h forecasts. Overall, as indicated by the rank based on the mean of relative errors of all forecast periods, the combination of YSU and Ferrier schemes provided the best prediction among all combinations, and thus we focus on this combination in the following analysis.

As an example, Fig. 2 shows the 6 hourly observed track as well as the 60-h forecast tracks and the TPEs by each combination of physical schemes starting at 0000 UTC July 22, 2012, for Typhoon Vicente (201208), which made landfall on the coast of south China. The forecast for the last 12 h is ignored because the real TC was dying out at this period. The combination of YSU and Ferrier schemes performs slightly better than most of the other combinations with the 48-h and 60-h forecast TPEs of 154.5 and 279.4 km, respectively, while it performs significantly better than others for the 24-h forecast with a TPE of 15.7 km. Although the combinations of the MYJ scheme with most microphysics

Table 1 Mean track position error (TPE, unit: km) and relative error (R_i) of 24-h, 48-h and 72-h forecasts as well as the rank for different combinations of three PBL schemes and four microphysics schemes, averaged over an ensemble of forecasts for five landed tropical cyclones during 2012

|	24-h		48-h		72-h		Mean		Rank
	TPE	R_i	TPE	R_i	TPE	R_i	TPE	R_i	
YSU_Ferrier	89.9	0.86	189.5	0.94	427.7	0.92	235.7	0.91	1
YSU_Goddard	132.1	1.26	235.5	1.17	476.2	1.03	281.3	1.15	12
YSU_WSM6	103.3	0.99	216.3	1.08	471.2	1.02	263.6	1.03	10
YSU_Lin	113.2	1.08	194.4	0.97	443.8	0.96	250.5	1.00	7
MYJ_Ferrier	98.4	0.94	192.9	0.96	438.0	0.95	243.1	0.95	2
MYJ_Goddard	104.3	1.00	196.2	0.98	480.2	1.04	260.2	1.00	8
MYJ_WSM6	101.4	0.97	203.9	1.01	455.1	0.98	253.5	0.99	6
MYJ_Lin	105.2	1.01	188.6	0.94	446.6	0.96	246.8	0.97	4
MYNN2_Ferrier	101.2	0.97	190.9	0.95	466.8	1.01	253.0	0.98	5
MYNN2_Goddard	101.9	0.97	206.4	1.03	490.6	1.06	266.3	1.02	9
MYNN2_WSM6	105.3	1.01	207.1	1.03	513.0	1.11	275.1	1.05	11
MYNN2_Lin	99.1	0.95	188.9	0.94	445.8	0.96	244.6	0.95	3
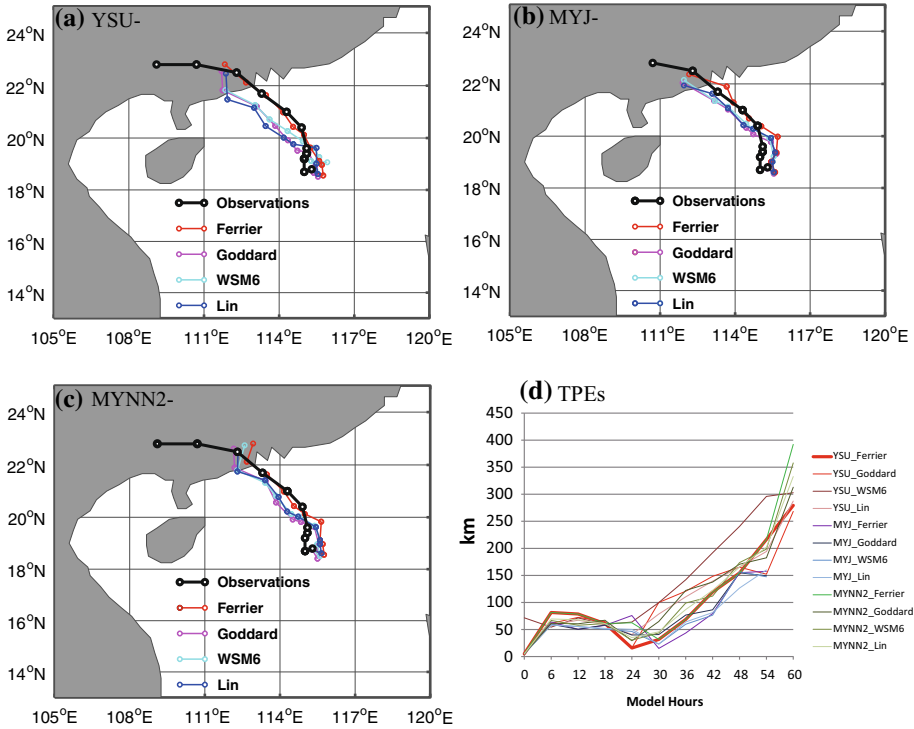
Fig. 2 Six hourly observed and the predicted tracks by combinations of different microphysics schemes with (**a**) YSU, (**b**) MYJ, (**c**) MYNN2 PBL schemes and (**d**) the track position errors (TPE, unit: km) for the 60-h forecast for Typhoon Vicnte (201208) started at 0000 UTC July 22, 2012

schemes perform well from the 30- to 54-h forecast, they do not work for the 60-h forecasts because the simulated vortexes are too weak, with their sintensity weaker than a tropical depression.

In the next two subsections, the reason why the combination of YSU and Ferrier schemes performed the best for TC track forecast is revealed from analyzing the steering flows and other atmospheric variables such as the 500-hPa geopotential height, 10-m winds and the water vapor distributions as well as the precipitation.

3.2 The steering flows

Previous studies (e.g., Holland 1983; Wu et al. 2005) have pointed out that TC tracks are strongly influenced by large-scale steering flows. Accurate prediction of steering flow would guarantee the accuracy of TC track prediction. Following this line, the biases of u- and v-components of the steering flows from the 72-h forecasts of each combination against the NCEP Final Analysis (FNL) are displayed in Fig. 3. The deep-layer mean steering flows are obtained through averaging the wind field between 925- and 300-hPa over a 3–8° radial band from TC center, based on the suggestions or experiences in previous studies (e.g., Chan and Gray 1982; Evans et al. 1991). Compared with other combinations, the combination of YSU and Ferrier schemes produces relatively small
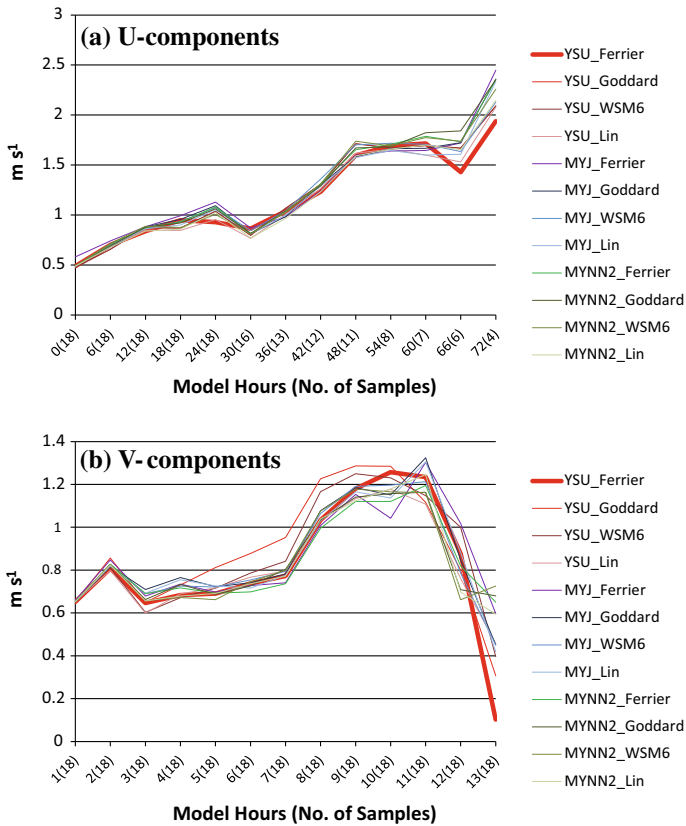
Fig. 3 Mean bias of (**a**) u- and (**b**) v-components of steering flow (unit: m s^{-1}) from the 72-h forecast by different combinations of three PBL schemes and four microphysics schemes, averaged over an ensemble of forecasts for five landed TCs during 2012

errors in both u- and v-components. This more accurate prediction of steering flows is beneficial to TC track forecasts.

Note that the combinations of YSU PBL scheme with other three microphysics schemes did not perform as well as the MYJ and MYNN2 PBL schemes (e.g., the v-components of the steering flows), suggesting that interactions between different PBL and microphysics schemes is an important factor of the predictions of TCs.

3.3 Atmospheric structures

Based on a spatial correlation analysis, the forecast 500-hPa geopotential height, 10-m winds and the water vapor distributions as well as the precipitation predicted by each combination of different PBL and microphysics schemes are compared with observations. Here, the spatial correlation coefficients between the FNL analysis and the forecast variables that interpolated onto the grids of FNL through averaging, are calculated within a fixed region (100–130°E, 0–30°N) covering the range of the five TCs. Examples for this interpolation are shown in Figs. 4b, 5b, 6b, respectively. Comparing the interpolated fields

Fig. 4 The 500-hPa geopotential height (unit: geopotential meters, GPM) by (**a**) the FNL analysis, (**b**) the interpolated fields from the forecast by the combination of YSU scheme and Ferrier scheme, and the original forecasts field by the combinations of (**c**) YSU and Ferrier schemes, (**d**) YSU and Goddard schemes, (**e**) YSU and WSN6 schemes, (**f**) YSU and Lin schemes, (**g**) MYJ and Ferrier schemes, as well as (**h**) MYNN2 and Ferrier schemes at the 30-h forecast time, valid at 0600 UTC July 23, 2012, for Typhoon Vicnte (201208) (*shaded area* for values larger than 5840 GPM in the FNL analysis, and for values larger than 5860 GPM in the model forecasts)
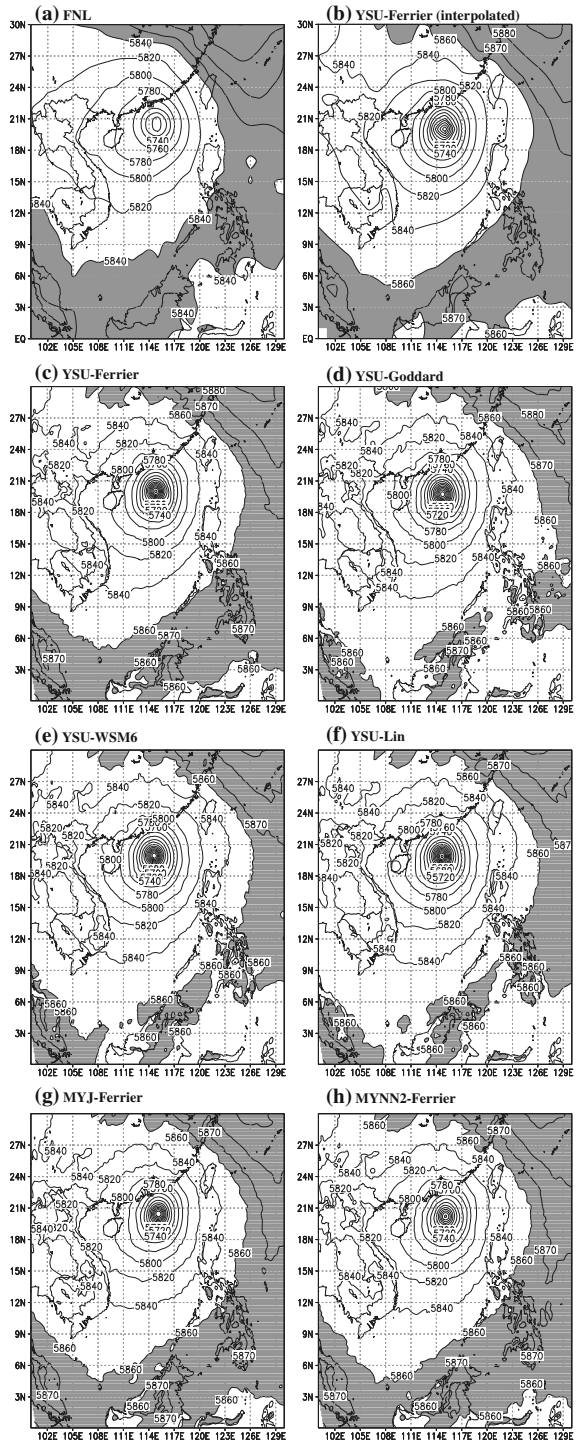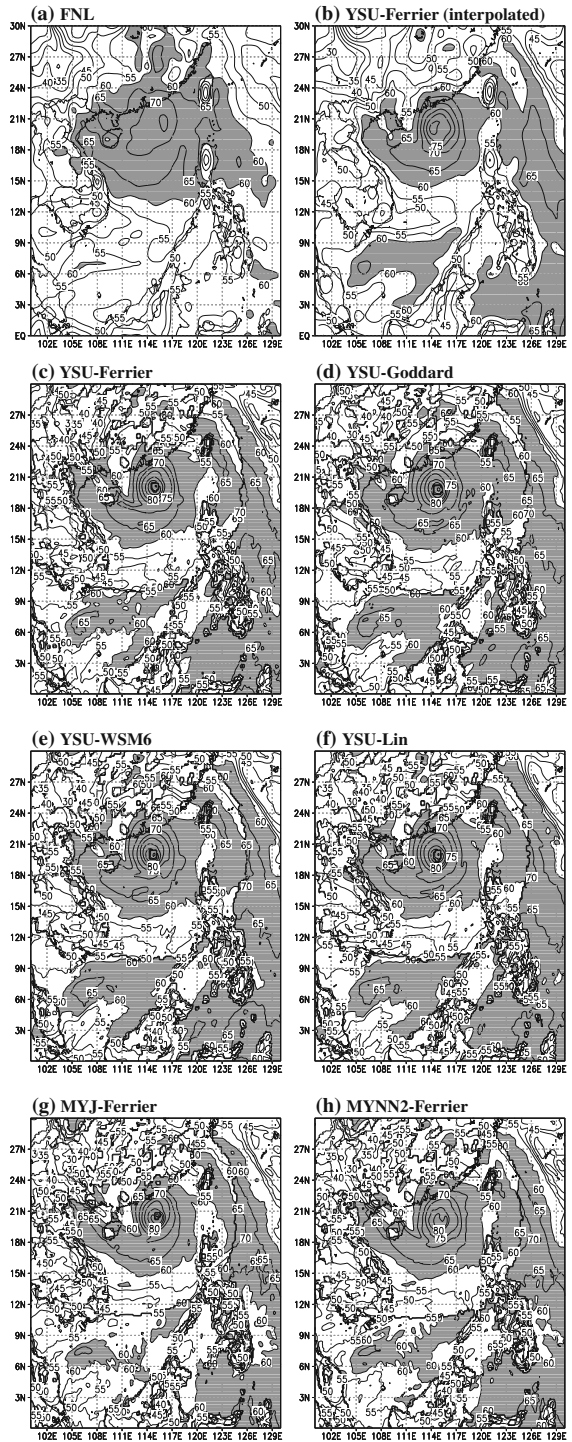
Fig. 5 Similar to Fig. 4, but for the 10-m winds (unit: m s^{-1}, *shaded area* for the magnitudes of the winds with an interval and minimum value of 5 m s^{-1})
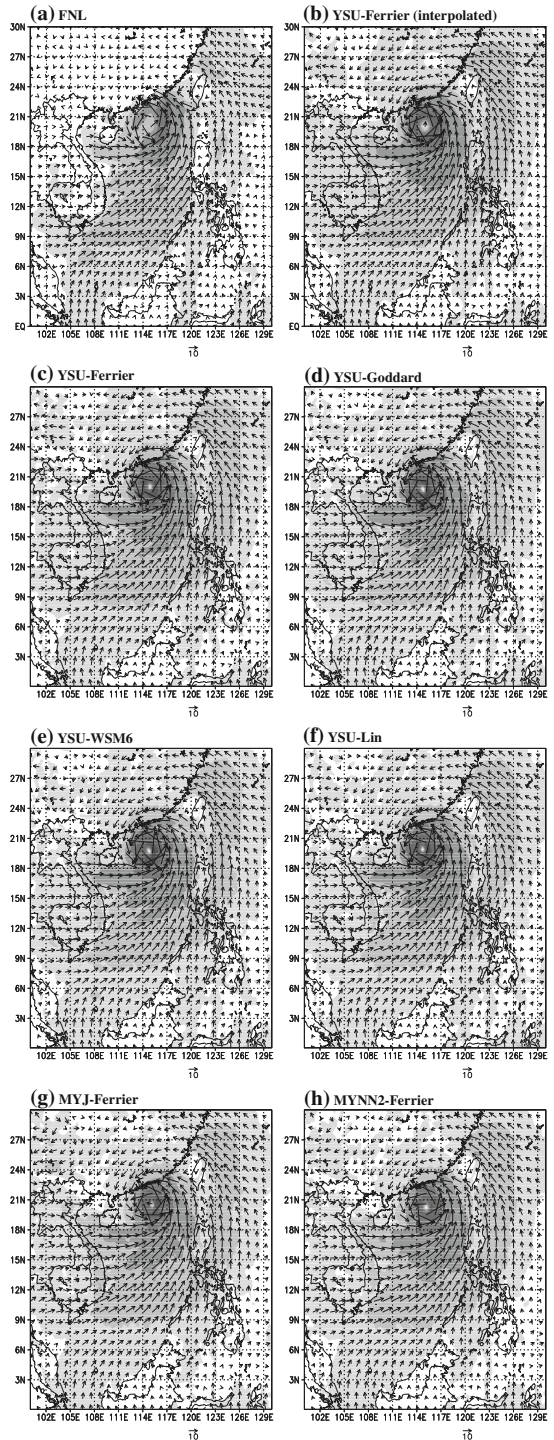
Fig. 6 Similar to Fig. 4, but for the precipitable water (unit: kg m^{-2}, *shaded area* for values larger than 60 kg m^{-2})

with the original fields, we can see that although small-scale features are filtered out by the interpolation, the general features are preserved, suggesting that the interpolated data are suitable for this spatial correlation analysis. Besides, in order to amplify the impacts of the PBL schemes, the correlation analysis is made at the moment right before the landing of TCs. Table 2 lists the coefficients averaged over the ensemble of forecasts for the five TCs.

The averaged spatial correlation coefficients for the 500-hPa geopotential height is shown in Table 2, showing that the combination of YSU and Ferrier schemes performs relatively better than other combinations with the coefficient of 8.97×10^{-1}. Concentrating on this combination, a comparison between the FNL analysis and the forecast field with other combinations including YSU scheme or Ferrier scheme is carried out. An example is shown in Fig. 4. The structure of the geopotential height over the SCS is dominant by two atmospheric systems, one is the subtropical high, which steers the TCs westward along its southwest flank, and the other is the structure of TC itself. Though all of the forecasts overestimate the magnitudes by about 20 GPM, the structure of the subtropical high is well predicted by the combination of YSU and Ferrier schemes, especially over the southeast part of the fixed region. The structures of TCs are similar between different combinations, suggesting that the combination of different PBL and microphysics schemes exert relatively fewer effects on the prediction of TC intensities.

As illustrated in Table 2, the combination of YSU and Ferrier schemes performs the best for the forecasts of v-components of the 10-m winds, and the second for those of the u-components. Because the position of TC center is also determined by the structure of surface winds, the well-predicted surface winds is beneficial to TC track forecasting. As shown in Fig. 5, the large-scale environment and the asymmetric structure of TC are well predicted by all of the combinations; however, the locations of the strong wind regions near the TC are mainly governed by the PBL schemes. For example, the strong wind region located south of the Hainan Island is absent in the forecasts by the MYJ and the MYNN2

Table 2 Spatial correlations between the FNL and the forecast 500-hPa height, 10-m winds and precipitable water by each combination of three PBL schemes and four microphysics schemes, averaged over an ensemble of forecasts for five landed TCs during 2012

	500-hPa height	10-m winds		Precipitable water
		U-components	V-components	
YSU_Ferrier	8.97×10^{-1}	8.27×10^{-1}	8.06×10^{-1}	8.17×10^{-1}
YSU_Goddard	8.87×10^{-1}	8.29×10^{-1}	8.06×10^{-1}	8.21×10^{-1}
YSU_WSM6	8.87×10^{-1}	8.28×10^{-1}	8.05×10^{-1}	8.23×10^{-1}
YSU_Lin	8.89×10^{-1}	8.27×10^{-1}	8.12×10^{-1}	8.23×10^{-1}
MYJ_Ferrier	8.89×10^{-1}	7.87×10^{-1}	7.83×10^{-1}	8.22×10^{-1}
MYJ_Goddard	8.95×10^{-1}	8.01×10^{-1}	7.96×10^{-1}	8.31×10^{-1}
MYJ_WSM6	8.95×10^{-1}	8.06×10^{-1}	7.95×10^{-1}	8.32×10^{-1}
MYJ_Lin	8.97×10^{-1}	8.00×10^{-1}	8.01×10^{-1}	8.33×10^{-1}
MYNN2_Ferrier	8.92×10^{-1}	8.11×10^{-1}	7.98×10^{-1}	8.25×10^{-1}
MYNN2_Goddard	8.91×10^{-1}	8.20×10^{-1}	8.02×10^{-1}	8.29×10^{-1}
MYNN2_WSM6	8.88×10^{-1}	8.27×10^{-1}	8.01×10^{-1}	8.30×10^{-1}
MYNN2_Lin	8.92×10^{-1}	8.22×10^{-1}	8.05×10^{-1}	8.31×10^{-1}

schemes, suggesting that the YSU scheme is beneficial to the forecasting of surface winds during TC's influence.

The combination of YSU and Ferrier schemes performs the last one for the forecast of the precipitable water (the total atmospheric water vapor contained in a vertical column of unit cross-sectional area) (Table 2). As shown in Fig. 6, the YSU scheme failed in forecasting the distributions of water vapor within the outer radii of TCs, as the sea area southeast to the Indo-China Peninsula is too wet; besides, the TCs simulated by the Ferrier scheme are relatively drier, as the shading areas in the combinations including the Ferrier scheme are relatively smaller than those in the combinations including other microphysics schemes. Figure 7 shows the comparison of the accumulated precipitation between the Tropical Rainfall Measuring Mission (TRMM) Microwave Imager (TMI) 3B42 and the combinations between the YSU
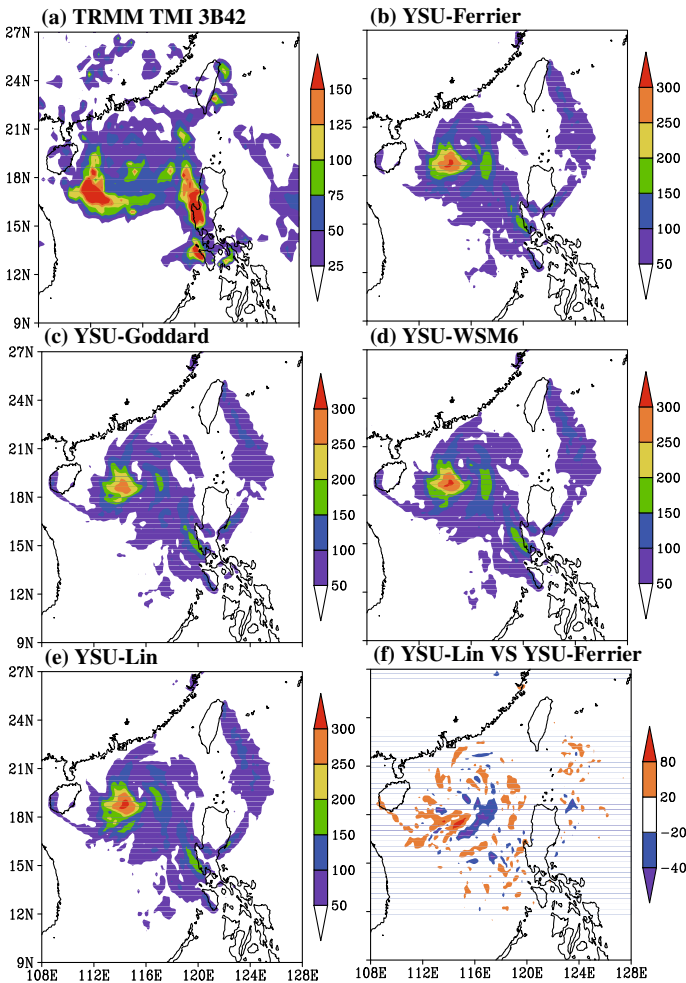
Fig. 7 The 30-h accumulated precipitation (mm) valid at 0600 UTC July 23, 2012, for Typhoon Vicnte (201208) by (**a**) Tropical Rainfall Measuring Mission (TRMM) Microwave Imager (TMI) 3B42, the combinations of YSU scheme and (**b**) Ferrier scheme, (**c**) Goddard scheme, (**d**) WSM6 scheme, and (**e**) Lin scheme, respectively. The difference between the combination of YSU and Lin schemes and the combination of YSU and Ferrier schemes is illustrated in (**f**)

scheme and different microphysics schemes. Although TRMM has superior skill in detecting TC heavy rains (Islam and Uyeda 2005; Chen et al. 2013), it tends to underestimate moderate to high rain (>50 mm h^{-1}). Hence, the simulated precipitations are almost double that of TRMM. The precipitation south of the Hainan Island is not well simulated by the Ferrier scheme. Compared to the Lin scheme (Fig. 7f), the Ferrier scheme simulates fewer precipitations, while the position of the precipitation cell is about $2°$ easterner. Overall, the forecast of the water vapor distributions and the precipitations by the combination of YSU and Ferrier schemes do not perform as well as that of the geopotential height and the surface winds. Since this combination preforms the best in track forecasting, the relationship between the distribution of precipitation and TC tracks is worth discussing.

4 Conclusions and discussion

An ensemble of forecasting experiments using different combinations of three PBL schemes (YSU, MYJ and MYNN2) and four microphysics schemes (Ferrier, Goddard, WSM6 and Lin) are carried out for five landed TCs during 2012. Among all the experiments, the combination of YSU scheme and Ferrier scheme performs the best for the forecast of TC tracks. A further analysis indicates that the combination of YSU Ferrier schemes produces a more accurate steering flow as well as TC wind structure, leading to a more accurate TC track forecast.

It is worth noting that, although the combination of YSU and Ferrier schemes performs the best for the forecast of TC tracks, it does not perform the best for the forecast of precipitation which is affected by a number of factors besides the PBL and microphysical schemes. Studies have found that it can be effectively improved by some techniques, including "optimizing" the initial conditions through data assimilation (Zhou et al. 2010; Zhang et al. 2013; Zheng et al. 2015), increasing the model resolution (De Bruijn and Brandsma 2000; Lonfat et al. 2007), and adopting a "best" cumulus parameterization scheme that takes into account the specific region and model resolution (Nasrollahi et al. 2012; Ma and Tan 2009).

Finally, it should be aware that the effects of the physical schemes on the forecasts of TCs may vary with different synoptic situations. More experiments with different combination of the physical schemes for the TC track forecast in different synoptic situations should be carried out in the future.

References

Chan JCL, Gray WM (1982) Tropical cyclone movement and surrounding flow relationships. Mon Wea Rev 110:1354–1374

Chen Y, Ebert EE, Walsh KJE, Davidson NE (2013) Evaluation of TRMM 3B42 precipitation estimates of tropical cyclone rainfall using PACRAIN data. J Geo Res 118:2184–2196. doi:10.1002/jgrd.50250

Chen S, Li W, Lu Y, Wen Z (2014) Variations of latent heat flux during tropical cyclones over the South China Sea. Meteorol Appl 21:717–723

De Bruijn EIF, Brandsma T (2000) Rainfall prediction for a flooding event in Ireland caused by the remnants of Hurricane Charley. J Hydrol 239:148–161

Dudhia J (1989) Numerical study of convection observed during the winter monsoon experiment using a mesoscale two-dimensional model. J Atmos Sci 46:3077–3107

Emanuel KA (2005) Increasing destructiveness of tropical cyclones over the past 30 years. Nature 436:686–688

Evans JL, Holland GL, Elsberry RL (1991) Interactions between a barotropic vortex and an idealized subtropical ridge. Part I: vortex Motion. J Atmos Sci 48:301–314

Ferrier BS, Lin Y, Black T, Rogers E, DiMego G (2002) Implementation of a new grid-scale cloud and precipitation scheme in the NCEP Eta model. Preprints, 15th conference on numerical weather prediction, San Antonio, TX, American Meteorological Society, pp 280–283

Holland GJ (1983) Tropical cyclone motion: environmental interaction plus a Beta effect. J Atmos Sci 40:328–342

Hong SY, Lim JOJ (2006) The WRF Single-Moment 6-Class microphysics scheme (WSM6). J Korean Meteor Soc 42:129–151

Hong SY, Noh Y, Dudhia J (2006) A new vertical diffusion package with an explicit treatment of entrainment processes. Mon Wea Rev 134:2318–2341

Islam MN, Uyeda H (2005) Comparison of TRMM 3B42 products with surface rainfall over Bangladesh. Proceedings in the IEEE international geoscience and remote sensing symposium (IGARSS05), Seoul:IEEE, 2005, pp 412–415

Janjić ZI (1994) The step-mountain eta coordinate model: further developments of the convection, viscous sublayer, and turbulence closure schemes. Mon Wea Rev 122:927–945

Kain JS, Fritsch JM (1990) A one-dimensional entraining/detraining plume model and its application in convective parameterization. J Atmos Sci 47:2784–2802

Kain JS, Fritsch JM (1993) Convective parameterization for mesoscale models: the Kain–Fritsch scheme, pp 165–170 in The representation of cumulus convection in numerical models, Emanuel KA, Raymond DJ (eds). Meteorol. Monogr. No. 46. American Meteorological Society

Kanada S, Wada A, Nakano M, Kato T (2012) Effect of planetary boundary layer schemes on the development of intense tropical cyclones using a cloud-resolving model. J Geo Res 117(D3). doi:10.1029/2011JD016582

Kepert JD (2012) Choosing a boundary layer parameterization for tropical cyclone modeling. Mon Wea Rev 140:1427–1445

Khain A, Lynn B (2011) Simulation of tropical cyclones using spectral bin microphysics, Recent Hurricane Research—Climate, Dynamics, and Societal Impacts, Prof. Anthony Lupo (ed). ISBN: 978-953-307-238-8, InTech

Lin YL, Farley RD, Orville HD (1983) Bulk parameterization of the snow field in a cloud model. J Clim Appl Meteor 22:1065–1092

Lonfat M, Rogers R, Marchok T, Marks JRFD (2007) A parametric model for predicting hurricane rainfall. Mon Wea Rev 135:3086–3094

Ma LM, Tan ZM (2009) Improving the behavior of the cumulus parameterization for tropical cyclone prediction: Convection trigger. Atmos Res 92:190–211

Mlawer EJ, Taubman SJ, Brown PD, Iacono MJ, Clough SA (1997) Radiative transfer for inhomogeneous atmosphere: RRTM, a validated correlated-k model for the longwave. J Geo Res 102(D14):16663–16682

Nakanishi M (2000) Large-eddy simulation of radiation fog. Bound-Layer Meteorol 94:461–493

Nakanishi M (2001) Improvement of the Mellor-Yamada turbulence closure model based on large-eddy simulation data. Bound-Layer Meteorol 99:349–378

Nakanishi M, Niino H (2004) An improved Mellor-Yamada level-3 model with condensation physics: its design and verification. Bound-Layer Meteorol 112:1–31

Nakanishi M, Niino H (2006) An improved Mellor-Yamada Level-3 Model: its numerical stability and application to a regional prediction of advection fog. Bound-Layer Meteorol 119:397–407

Nasrollahi N, AghaKouchak A, Li J, Gao X, Hsu K, Sorooshian S (2012) Assessing the impacts of different WRF precipitation physics in hurricane simulations. Wea Forecast 27:1003–1016

Neumann CJ, Pelissier JM (1981) An analysis of Atlantic tropical cyclone forecast errors, 1970–1979. Mon Wea Rev 109:1248–1266

Pattanayak S, Mohanty UC, Osuri KK (2012) Impact of parameterization of physical processes on simulation of track and intensity of Tropical Cyclone Nargis (2008) with WRF-NMM Model. The Scientific World Journal, 2012. Article ID 671437

Peng S, Qian YK, Lai Z, Hao S, Chen S, Xu H, Wang D, Xu X, Chan JCL, Zhou H, Liu D (2014) On the mechanisms of the recurvature of super typhoon megi. Sci Rep 4(4451). doi:10.1038/srep04451

Powell MD, Aberson SD (2001) Accuracy of United States tropical cyclone landfall forecasts in the Atlantic basin (1976–2000). Bull Am Meteor Soc 82:2749–2768

Rao DVB, Prasad DH (2007) Sensitivity of tropical cyclone intensification to boundary layer and convective processes. Nat Hazards 41:429–445

Skamarock WC, Klemp JB, Dudhia J, Gill DO, Barker DM, Duda MG, Huang X, Wang W, Powers JG (2008) A description of the advanced research WRF version 3, 113 pp. http://www.mmm.ucar.edu/wrf/users/docs/arw_v3.pdf

Tao WK, Simpson J, McCumber M (1989) An ice-water saturation adjustment. Mon Wea Rev 117:231–235

Wang Y (2002) An explicit simulation of tropical cyclones with a triply nested movable wesh primitive equation model: TCM3. part II: model refinements and sensitivity to cloud microphysics parameterization. Mon Wea Rev 130:3022–3036

Wu L, Wang B, Geng S (2005) Growing typhoon influence on east Asia. Geo Res Lett 32(18). doi:10.1029/2005GL022937

Zhang M, Zupanski M, Kim MJ (2013) Assimilating AMSU-A radiances in the TC core area with NOAA operational HWRF (2011) and a hybrid data assimilation system: Danielle (2010). Mon Wea Rev 141:3889–3907

Zheng J, Li J, Schmit TJ, Li J, Liu Z (2015) The impact of AIRS atmospheric temperature and moisture profiles on hurricane forecasts: Ike (2008) and Irene (2011). Adv Atmos Sci 32:319–335

Zhou YP, Lau KM, Reale O, Rosenberg R (2010) AIRS impact on precipitation analysis and forecast of tropical cyclones in a global data assimilation and forecast system. Geo Res Lett 37:L02806. doi:10.1029/2009GL041494

Zhou H, Zhu W, Peng S (2013) The impacts of different micro-physics schemes and boundary layer schemes on the simulated track and intensity of super typhoon Megi (1013). J Tropical Meteo 28:599–608 (in Chinese)